Title	Compact photoacoustic tomography system
Author(s)	Kalva, Sandeep Kumar; Pramanik, Manojit
Citation	Kalva, S. K., & Pramanik, M. (2017). Compact photoacoustic tomography system. Proceedings of SPIE - Photons Plus Ultrasound: Imaging and Sensing 2017, 10064, 100643X-.
Date	2017
URL	http://hdl.handle.net/10220/44307
Rights	© 2017 Society of Photo-Optical Instrumentation Engineers (SPIE). This paper was published in Proceedings of SPIE - Photons Plus Ultrasound: Imaging and Sensing 2017 and is made available as an electronic reprint (preprint) with permission of Society of Photo-Optical Instrumentation Engineers (SPIE). The published version is available at: [http://dx.doi.org/10.1117/12.2250493]. One print or electronic copy may be made for personal use only. Systematic or multiple reproduction, distribution to multiple locations via electronic or other means, duplication of any material in this paper for a fee or for commercial purposes, or modification of the content of the paper is prohibited and is subject to penalties under law.

Compact photoacoustic tomography system

Sandeep Kumar Kalva, Manojit Pramanik*
School of Chemical and Biomedical Engineering, Nanyang Technological University, 62 Nanyang Drive, Singapore 637459

ABSTRACT

Photoacoustic tomography (PAT) is a non-ionizing biomedical imaging modality which finds applications in brain imaging, tumor angiogenesis, monitoring of vascularization, breast cancer imaging, monitoring of oxygen saturation levels etc. Typical PAT systems uses Q-switched Nd:YAG laser light illumination, single element large ultrasound transducer (UST) as detector. By holding the UST in horizontal plane and moving it in a circular motion around the sample in full 2π radians photoacoustic data is collected and images are reconstructed. The horizontal positioning of the UST make the scanning radius large, leading to larger water tank and also increases the load on the motor that rotates the UST. To overcome this limitation, we present a compact photoacoustic tomographic (ComPAT) system. In this ComPAT system, instead of holding the UST in horizontal plane, it is held in vertical plane and the photoacoustic waves generated at the sample are detected by the UST after it is reflected at 45^0 by an acoustic reflector attached to the transducer body. With this we can reduce the water tank size and load on the motor, thus overall PAT system size can be reduced. Here we show that with the ComPAT system nearly similar PA images (phantom and *in vivo* data) can be obtained as that of the existing PAT systems using both flat and cylindrically focused transducers.

Keywords: acoustic reflector, photoacoustic tomography, small animal imaging

1. INTRODUCTION

Photoacoustic tomography (PAT) is an evolving biomedical imaging modality that combines the rich optical contrast and high ultrasonic resolution.[1-8] A pulsed non-ionizing laser is used to irradiate the biological tissue. The light energy absorbed by the tissue results in rise of local temperature which results in thermoelastic expansion of tissue and finally the pressure waves known as photoacoustic (PA) waves are generated. These PA waves are acquired using an ultrasound transducer (UST).Various reconstruction algorithm are used to reconstruct the initial pressure map.[9-14] Deeper penetration imaging is possible in PAT which is shallow in other optical imaging techniques like optical coherence tomography and as ultrasound scattering is two to three orders of magnitude less than optical scattering, PAT gives better resolutions compared to optical imaging techniques. PAT has wide range of clinical applications like brain imaging,[15] breast cancer imaging,[16, 17] sentinel lymph node imaging,[18, 19] molecular imaging,[20] temperature monitoring and so on.[21-24]

Different types of transducers can be used in PAT system like single element UST,[9] linear array type,[19, 25] semi-circular array type[26] and circular array type of transducers.[27] Usage of single element USTs makes the PAT data acquisition slow whereas array types of transducers are faster in data acquisition. But array types of transducers are expensive and require multiple channel parallel amplification and data acquisition systems. As single element USTs are cheap and require only single amplifier and single channel data acquisition system, they are used in high speed PAT imaging systems like PLD-PAT system[28] and slip-ring based PAT system.[29]

In any PAT system, the single element UST is used in horizontal plane where the UST the UST is held in perpendicular to the laser illumination and facing towards the scanning center. This configuration results in more occupation of space by the water tank. Water tank houses the UST and the sample for providing better acoustic coupling.

* Email: manojit@ntu.edu.sg

Photons Plus Ultrasound: Imaging and Sensing 2017, edited by Alexander A. Oraevsky, Lihong V. Wang, Proc. of SPIE Vol. 10064, 100643X · © 2017 SPIE · CCC code: 1605-7422/17/$18 · doi: 10.1117/12.2250493

Here, we propose a novel Compact Photoacoustic Tomography (ComPAT) system, to use the UST in vertical position instead of placing it in horizontal direction. The generated pressure waves are guided to the transducer detector area by using an acoustic reflector [made of stainless steel: Fig. 1(b)] placed at 45^0 to the UST surface. This placement of the UST in vertical position makes the tank size small and the load on the motor also reduces. So the entire PAT system can be minimized. In this paper we have conducted studies on *in vitro* chicken breast tissue phantom and *in vivo* small animals and shown that we get similar quality images using UST with reflector (USTR) as those of conventional UST for both flat and cylindrically focused transducers. We have used simple delay-and-sum reconstruction algorithm to reconstruct PA images.

2. EXPERIMENTS AND RESULTS

Optical Parametric Oscillator (OPO) laser pumped by Q-switched Nd:YAG (Continuum, Surelite Ex; 532 nm) laser was used to deliver 680 nm pulsed laser of 5 ns pulse width at 10Hz frequency. The laser energy density was ~6 mJ/cm^2 which is much below the ANSI safety limit[30] of 20 mJ/cm^2 at 400-700 nm. Figure 1 shows the schematic set up of the PAT imaging system.

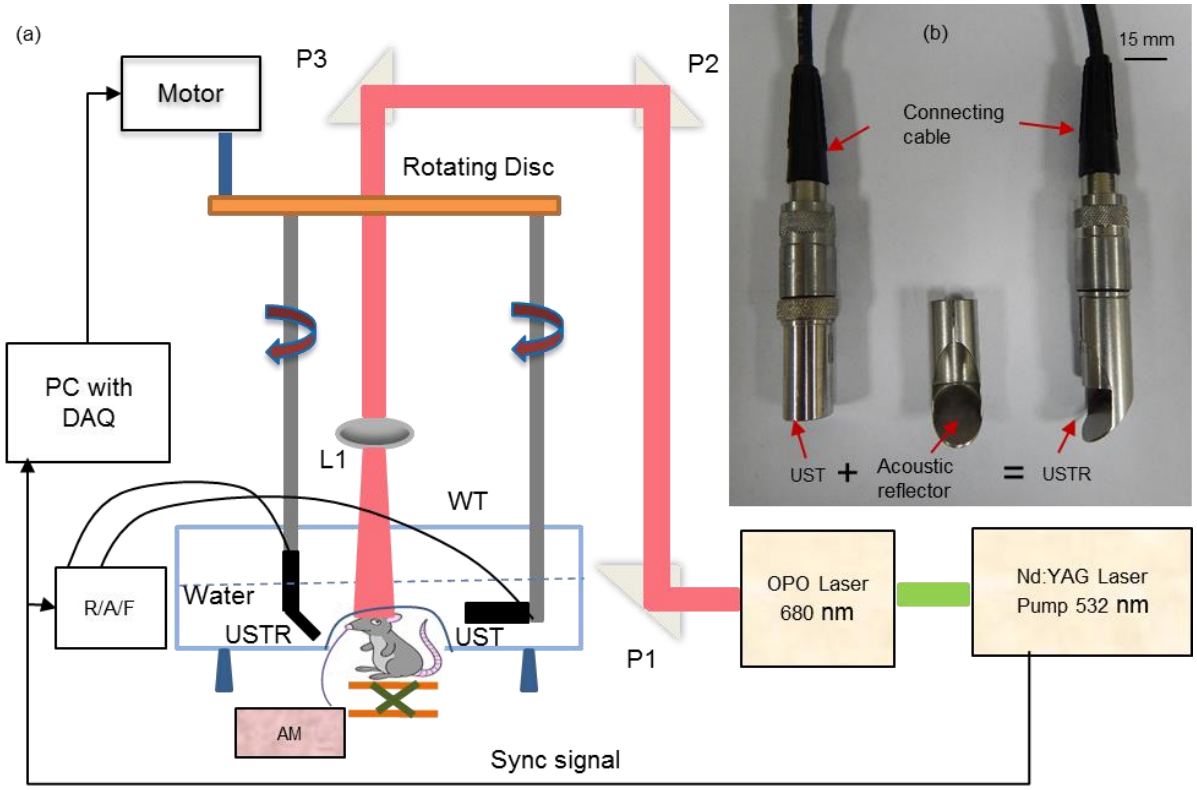

Fig. 1 (a) Schematic diagram of the PAT set up. P1, P2, P3: coated prisms; DAQ: Data Acquisition card; R/A/F: Receiver/Amplifier/Filter; UST: Ultrasound Transducer; USTR: Ultrasound transducer with reflector; WT: Water tank; L1: Plano concave lens; AM: Anesthetizing Machine. (b) Image of conventional UST and acoustic reflector attached to the conventional UST.

The UST moves around the target object in a full 360^0 rotation to acquire PA data. We have used flat UST (Olympus NDT, V306-SU), a flat USTR (acoustic reflector: F102, Olympus NDT attached to flat UST), focused UST

(Olympus NDT, V306-SU-NK, CF = 1.90 inch) and focused USTR (acoustic reflector F102, Olympus NDT attached to focused UST) for PA data acquisition. The USTs have a central frequency of 2.25 MHz with ~70% nominal bandwidth and 13 mm diameter detection area. The PA signals were collected continuously for 60 sec with UST moving around the target object at a rotational speed of 6 degrees/sec. All the acquired PA signal were regrouped into 200 A-lines. The acquired PA signals were amplified and filtered using a pulse amplifier (Olympus-NDT, 5072PR) and stored into a desktop (Intel 3.7GHz, 64-bit processor, 16 GB RAM, Win 10 OS) using data acquisition (DAQ) card (GaGe compuscope 4227).

A study was conducted using 'N' shaped blood vessel phantom made of low density polyethylene (LDPE) tubes of 0.38 mm inner diameter embedded inside chicken breast tissue [Fig. 2 (a)]. The tubes phantom was of ~1 cm x 1 cm dimensions [Fig. 2 (a) - inset]. One more layer of chicken tissue (~5 mm thick) was placed on top. The reconstructed cross sectional PA images are shown in Figs. 2 (b), (c) were obtained using flat UST and flat USTR, respectively and Figs. 2 (d), (e) were obtained using focused UST and focused USTR. From the reconstructed images, it is clearly seen that we get similar images using acoustic reflector augmented to the UST as those of the images obtained using conventional UST for both flat and focused transducers. The SNR was calculated to be 22.4 dB for flat UST and 24.23 dB for flat USTR. The SNR levels for focused UST and focused USTR were 20.38 dB and 21.7 dB respectively.

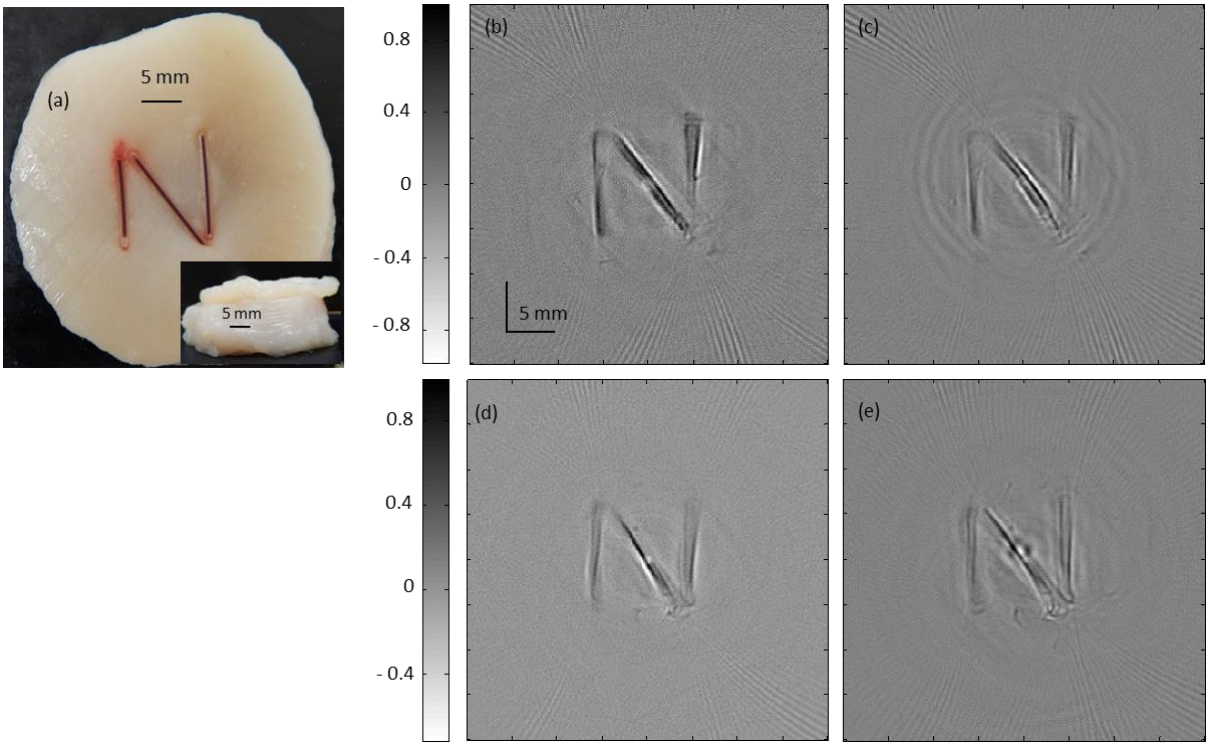

Fig. 2 (a) 'N' shaped blood vessel phantom embedded inside chicken breast tissue (inset: one more layer of 5 mm thick chicken breast tissue placed on top). (b), (c) reconstructed PA images obtained using flat UST and flat USTR respectively. (d), (e) reconstructed PA images obtained using focused UST and focused USTR respectively.

Next, *in vivo* animal experiments were conducted using healthy female rats weighing approximately 120 gm procured from InVivos Pte. Ltd., Singapore. All the animal experiments were perfumed according to the approved

guidelines and regulations by the institutional Animal Care and Use committee of Nanyang Technological University, Singapore (Animal Protocol Number ARF-SBS/NIE-A0263). Before the experiments, animals were anesthetized using the anesthetic cocktail containing Ketamine and Xylazine of 120 mg/Kg and 16 mg/Kg respectively. The anesthesia was injected intraperitoneally into the animal's body with a dosage of 0.2 ml/ 100 gm. The animal's head was trimmed and then epilated using hair removal cream. The animal was placed on its abdomen in sitting position on a customized animal holder. Animal along with animal holder were mounted on a translational stage. After placing the animal in the PAT scanning region, a breathing mask covering the nose and mouth of the animal was used to deliver anesthesia mixture of O_2 and isoflurane during imaging. The translational stage was adjusted to position the animal's head in the center of the scanning system. After the data acquisition, animals were euthanized by injecting Valabarb (sodium pentobarbitone 300 mg/ml) intraperitoneally.

The reconstructed cross-sectional PA images of animal brain are shown in Fig. 3. Figures 3(a) and 3(b) are the reconstructed images obtained using flat UST and flat USTR. Figures 3(c) and 3(d) are the reconstructed images obtained using focused UST and focused USTR. As can be observed from the images, that using acoustic reflector augmented to the UST, we get similar images as those from the conventional UST.

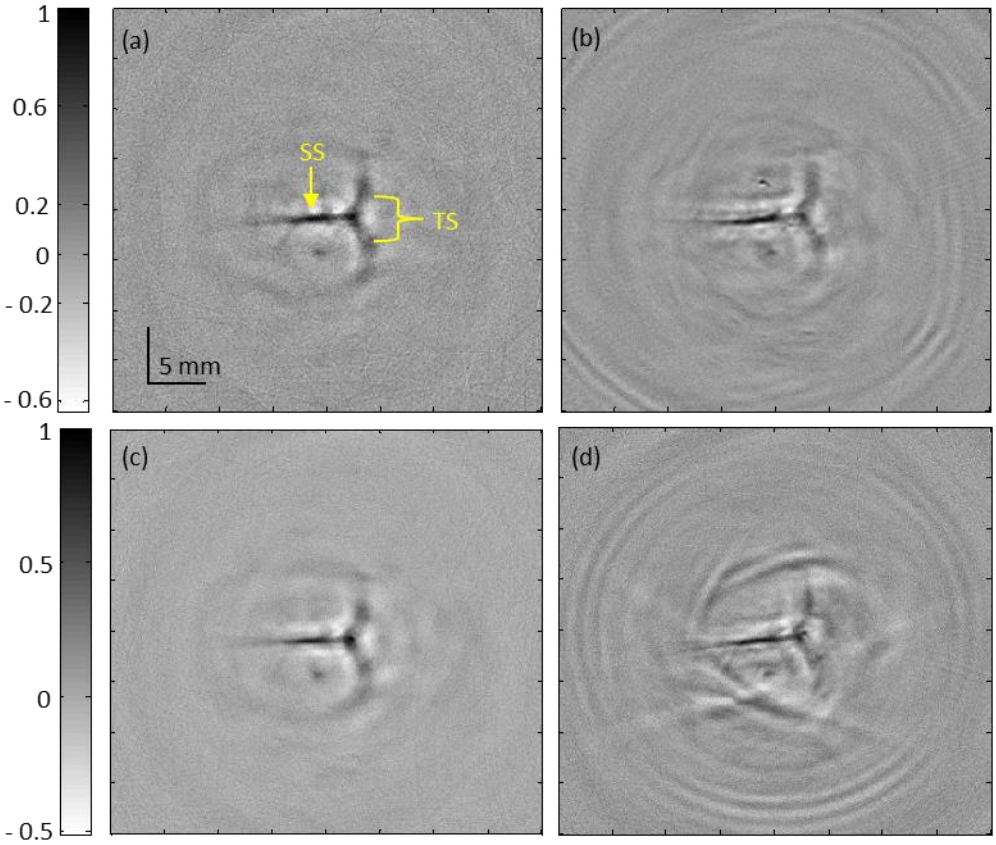

Fig. 3 *In vivo* rat brain images. (a) and (b) Reconstructed PA images obtained using flat UST and flat USTR, respectively. (c) and (d) Reconstructed PA images obtained using focused UST and focused USTR. SS: superior Sagittal Sinus; TS: Transverse Sinus.

In all these images, the superior sagittal sinus (SS) and transverse sinuses (TS) of the rat brain are clearly visible. The images obtained using acoustic reflector augmented to the conventional UST are almost similar to that of the images

obtained using conventional UST. The SNR was calculated to be 17.1 dB for flat UST and 22.2 dB for flat USTR. The SNR levels were 18.21 dB for focused UST and 14.65 dB for focused USTR.

The acoustic reflector was placed at 45^0 to the transducer body. The ultrasound waves reaching the reflector surface will fall at 45^0 to the water and reflector interface. At this incidence angle, total internal reflection phenomena occurs and ultrasound waves will be fully reflected back into the water medium which are detected by the transducer. The SNR levels were maintained though there was some ~6-29% enhancement or degradation. This change was due to the small difference (~2-4 mm) in the UST and USTR positioned from the scanning center. Amplitude of the PA signal is inversely proportional to the distance at which the target object is placed form the transducer.SO there were small variations in the SNR levels. If the transducers are kept exactly at same distance from the scanning center then similar SNR levels can be maintained.

3. CONCLUSIONS

In this work, we showed that by using an acoustic reflector made of stainless steel augmented to the conventional UST, we get similar quality PA images as that of the images obtained using conventional UST for both flat and focused transducers. The results obtained using chicken breast tissue phantoms and *in vivo* animal images support that the vertical configuration of the UST makes the PAT imaging system more compact and also portable.

ACKNOWLEDGEMENT

This research is supported by the Singapore Ministry of Health's National Medical Research Council (NMRC/OFIRG/0005/2016: M4062012). Authors have no relevant financial interests in the manuscript and no other potential conflicts of interest to disclose.

REFERENCES

[1] Upputuri, P. K., and Pramanik, M., "Recent advances toward preclinical and clinical translation of photoacoustic tomography: a review," Journal of Biomedical Optics, 22(4), 041006 (2017).
[2] Zhou, Y., Yao, J., and Wang, L. V., "Tutorial on photoacoustic tomography," Journal of Biomedical Optics, 21(6), 061007 (2016).
[3] Wang, L. V., and Yao, J., "A practical guide to photoacoustic tomography in the life sciences," Nat Methods, 13(8), 627-38 (2016).
[4] Upputuri, P. K., Sivasubramanian, K., Mark, C. S. K. *et al.*, "Recent Developments in Vascular Imaging Techniques in Tissue Engineering and Regenerative Medicine," BioMed Research International, 2015, 9 (2015).
[5] Wang, L. V., and Hu, S., "Photoacoustic Tomography: In Vivo Imaging from Organelles to Organs," Science, 335(6075), 1458-1462 (2012).
[6] Wang, L. V., "Multiscale photoacoustic microscopy and computed tomography," Nature Photonics, 3(9), 503-509 (2009).
[7] Li, C., and Wang, L. V., "Photoacoustic tomography and sensing in biomedicine," Physics in Medicine and Biology, 54(19), R59-97 (2009).
[8] Wang, L. V., "Prospects of photoacoustic tomography," Medical Physics, 35(12), 5758-67 (2008).
[9] Kalva, S. K., and Pramanik, M., "Experimental validation of tangential resolution improvement in photoacoustic tomography using a modified delay-and-sum reconstruction algorithm," Journal of Biomedical Optics, 21(8), 086011 (2016).

[10] Prakash, J., Raju, A. S., Shaw, C. B. *et al.*, "Basis pursuit deconvolution for improving model-based reconstructed images in photoacoustic tomography," Biomed Opt Express, 5(5), 1363-77 (2014).
[11] Pramanik, M., "Improving tangential resolution with a modified delay-and-sum reconstruction algorithm in photoacoustic and thermoacoustic tomography," Journal of the Optical Society of America A, 31(3), 621-7 (2014).
[12] Shaw, C. B., Prakash, J., Pramanik, M. *et al.*, "Least squares QR-based decomposition provides an efficient way of computing optimal regularization parameter in photoacoustic tomography," Journal of Biomedical Optics, 18(8), 080501 (2013).
[13] Xu, M., and Wang, L. V., "Universal back-projection algorithm for photoacoustic computed tomography," Physical Review E, 71(1), 016706 (2005).
[14] Xu, Y., Xu, M. H., and Wang, L. V., "Exact frequency-domain reconstruction for thermoacoustic tomography - II: Cylindrical geometry," IEEE Transactions on Medical Imaging, 21(7), 829-833 (2002).
[15] Yang, X., and Wang, L. V., "Monkey brain cortex imaging by photoacoustic tomography," Journal of Biomedical Optics, 13(4), 044009 (2008).
[16] Song, N., [Quantitative photoacoustic tomography for breast cancer screening] Ecole Centrale Marseille, (2014).
[17] Ermilov, S. A., Khamapirad, T., Conjusteau, A. *et al.*, "Laser optoacoustic imaging system for detection of breast cancer," Journal of Biomedical Optics, 14(2), 024007 (2009).
[18] Garcia-Uribe, A., Erpelding, T. N., Krumholz, A. *et al.*, "Dual-Modality Photoacoustic and Ultrasound Imaging System for Noninvasive Sentinel Lymph Node Detection in Patients with Breast Cancer," Scientific Reports, 5, 15748 (2015).
[19] Erpelding, T. N., Kim, C., Pramanik, M. *et al.*, "Sentinel Lymph Nodes in the Rat : Noninvasive Photoacoustic and US imaging with a clinical US system," Radiology, 256(1), 102-110 (2010).
[20] Yao, J., Xia, J., and Wang, L. V., "Multiscale Functional and Molecular Photoacoustic Tomography," Ultrason Imaging, 38(1), 44-62 (2016).
[21] Daoudi, K., van den Berg, P. J., Rabot, O. *et al.*, "Handheld probe integrating laser diode and ultrasound transducer array for ultrasound/photoacoustic dual modality imaging," Optics Express, 22(21), 26365-74 (2014).
[22] Cai, X., Kim, C., Pramanik, M. *et al.*, "Photoacoustic tomography of foreign bodies in soft biological tissue," Journal of Biomedical Optics, 16(4), 046017 (2011).
[23] Pramanik, M., and Wang, L. V., "Thermoacoustic and photoacoustic sensing of temperature," Journal of Biomedical Optics, 14(5), 054024 (2009).
[24] Ku, G., Wang, X. D., Xie, X. Y. *et al.*, "Imaging of tumor angiogenesis in rat brains in vivo by photoacoustic tomography," Applied Optics, 44(5), 770-775 (2005).
[25] Wang, X., Fowlkes, J. B., Cannata, J. M. *et al.*, "Photoacoustic imaging with a commercial ultrasound system and a custom probe," Ultrasound in Medicine & Biology, 37(3), 484-92 (2011).
[26] Buehler, A., Deán-Ben, X. L., Claussen, J. *et al.*, "Three-dimensional optoacoustic tomography at video rate," Optics Express, 20(20), 22712-19 (2012).
[27] Li, C., Aguirre, A., Gamelin, J. *et al.*, "Real-time photoacoustic tomography of cortical hemodynamics in small animals," Journal of Biomedical Optics, 15(1), 010509 (2010).
[28] Upputuri, P. K., and Pramanik, M., "Performance characterization of low-cost, high-speed, portable pulsed laser diode photoacoustic tomography (PLD-PAT) system," Biomedical Optics Express, 6(10), 4118-29 (2015).
[29] Deng, Z., Li, W., and Li, C., "Slip-ring-based multi-transducer photoacoustic tomography system," Optics Letters, 41(12), 2859-62 (2016).
[30] "American National Standard for Safe Use of Lasers ANSI Z136.1-2000 (American National Standards Institute, Inc., New York, NY, 2000)."